IJE TRANSACTIONS A: Basics Vol. 31, No. 10, (October 2018) 1689-1697

International Journal of Engineering

Journal Homepage: www.ije.ir

Improvement Performances of Active and Reactive Power Control Applied to DFIG for Variable Speed Wind Turbine Using Sliding Mode Control and FOC

T. Douadi*[a], Y. Harbouche[a], R. Abdessemed[a], I. Bakhti[b]

[a] LEB – Research Laboratory, Department of Electrical Engineering, Mostefa Benboulaid-Batna 2 University, Algeria
[b] Laboratory of Electromagnetic Induction and Propulsion Systems, Department of Electrical Engineering, Batna University, Algeria

PAPER INFO

Paper history:
Received 08 April 2018
Received in revised form 26 July 2018
Accepted 17 August 2018

Keywords:
Doubly Fed Induction Generator
Field Oriented Control
Indirect Sliding Mode
Wind Energy
Pulse with Modulation PWM

ABSTRACT

This paper deals with the Active and Reactive Power control of double-fed induction generator (DFIG) for variable speed wind turbine. For controlling separately the active and the reactive power generated by a DFIG, field oriented control (FOC) and indirect sliding mode control (ISMC) are presented. These non linear controls are compared on the basis of topology, cost, efficiency. The main contribution of this work based to the short time of response with excellent convergence and high decoupled between active and reactive power in one part and in the second part we define the benefit to use indirect model of DFIG to the conception of indirect sliding mode control by using the relationships between stator powers and rotor currents. The simulation results have shown good performances concerning the tracking of the references both in transient and steady state and prove the effectiveness of sliding mode control to track the given references using PWM inverter.

***doi**: 10.5829/ije.2018.31.10a.11*

NOMENCLATURE

s, r	Stator and rotor subscripts.	S_w	Wind turbines blades swept area
R_s , R_r	Stator and rotor resistances (Ω)	C_{pmax}	Maximum power coefficient
L_s , L_r	Self inductance of stator and rotor (H)	G	Mechanical speed multiplier (gearbox)s
M	Is mutual magnetizing inductance.	Ω_t	Wind turbine angular speed (shaft speed) (rad/s)
J	Inertia moment of the moving element (kgm^2)	Ω	Mechanical speed (rad/s)
f	Viscous friction and iron-loss coefficient.	ω_r	Electrical angular rotor speed(rad/s)
ϕ_s , ϕ_r	Stator and rotor flux (Wb)	S_w	Wind turbines blades swept area
C_t	Wind turbine torque (Nm)	ω_s	Synchronously rotating angular speed (rad/s)
T_e	Electromagnetic torque (Nm)	V_s V_r	Stator and rotor voltage (V)
T_l	Load torque (N.m)	I_{ds},I_{qs}	Direct and quadrature component of the stator currents (A)
V	Wind speed (m/s)	I_{dr},I_{qr}	Direct and quadrature component of the rotor currents (A)
R	Blade radius (m)	P	Active power (W)
p	Number of pair poles	Q	Reactive power (VAR)
C_p	Power coefficient	g	Slip
Greek Symbols		λ	Ratio of the tip speed
ρ	Air density	MPPT	Maximum power point tracking
β	Pitch angle	ISMC	Indirect sliding mode control
Abbreviations		FOC	Field oriented control
MPPT	Maximum power point tracking	PWM	Pulse-width modulation
DFIG	Double fed induction generators		

*Corresponding Author Email: *tarek_douadi@hotmail.ca* (T. Douadi)

Please cite this article as: T. Douadi, Y. Harbouche, R. Abdessemed, I. Bakhti, Improvement Performances of Active and Reactive Power Control Applied to DFIG for Variable Speed Wind turbine using Sliding Mode Control and FOC, International Journal of Engineering (IJE), IJE TRANSACTIONS A: Basics Vol. 31, No. 10, (October 2018) 1689-1697

1. INTRODUCTION

In addition to other renewable energy sources, the wind energy is proving to be one of the preferred choices to produce electricity [1]. Among these sources of energy, the generators wind turbines occupy a special place.

Currently most wind turbines are equipped of a DFIG, this is due to several advantages: the variable speed generation (± 30% around the speed synchronism), the decoupled control of the powers active and reactive, reducing mechanical stress and acoustic noise, the improvement of power quality and low cost [1-4].

To have a good quality of electric power produced by a wind system based on an double fed induction generators, it is necessary to apply adequate techniques of control. The active power will be converge to their reference generated by the turbine to ensure a better output of the wind system and in the other hand the reactive power will be maintained null in order to keep a unit power-factor on stator side.

For improvement of performance for active and reactive power control there exist many kind of non linear controls. Vector control approaches present their ability to make the decoupled model of the DFIG [4]. However vector control approach exhibits low performance and less robustness when the DFIG nonlinearities are considered. To obtain high performances, the application of a robust control approach occupying a significant place among the robust controls named by Sliding Mode is presented in this paper.

Sliding mode control experienced a great success in recent years. This is due to the simplicity of its implementation and robustness compared to uncertainties of the system and external disturbances staining the process, this control law is the subject of several research works (example in electric traction, Aeronautics); the common advantage can be used alone or in hybrid controls with other control techniques [5-7]. The sliding mode control is to bring back the state trajectory to the sliding surface and the evolve on it with a certain dynamic to the balanced point [8, 9].

We can organize this paper as follows; modeling turbine is reviewed in section 2. Modeling of the DFIG in section 3. The Field Oriented control of DFIG are discussed and mentioned in section 4, section 5 is designed for Indirect sliding mode control deals with the simulation results. Finally, we present the conclusion of this work end the paper.

2. MODEL OF TURBINE

The wind turbine input power is:

$$P_v = \frac{1}{2}\rho S_w V^3 \quad (1)$$

where, ρ is air density, S_w is wind turbine blades swept area in the wind, V is wind speed.
The output mechanical power of wind turbine is:

$$P_m = C_p P_v = \frac{1}{2} C_p \rho S_w V^3 \quad (2)$$

where, C_p represents the wind turbine power conversion efficiency. It is a function of the tip speed ratio and the blade pitch angle β in a pitch-controlled wind turbine. λ is defined as the ratio of the tip speed of the turbine blades to wind speed:

$$\lambda = \frac{R.\Omega_t}{v} \quad (3)$$

where, R is blade radius. Ω is angular speed of the turbine. C_p can be described as [7]:

$$C_p(\beta,\lambda) = \left(0.5 - 0.0167.(\beta-2)\right).\sin\left(\frac{\pi.(\lambda+0.1)}{18.5-0.3.(\beta-2)}\right) - 0.00184.(\lambda-3).(\beta-2) \quad (4)$$

According to the Figure 1, we note that the increase the speed of the wind implies an increase the speed of the turbine, however this increase the power coefficient C_p maintains at its maximum value which explains the robustness of order MPPT. In our work we use the wind profile, as shown in Figure 2. Figure 3 present the mechanical speed and power its cleary shown the same profile of wind speed.

3. DFIG MODEL

Using Park transformation DFIG model is given by the following equations:

$$\begin{aligned} V_{ds} &= R_s I_{ds} + \frac{d}{dt}\phi_{ds} - \omega_s \phi_{qs} \\ V_{qs} &= R_s I_{qs} + \frac{d}{dt}\phi_{qs} + \omega_s \phi_{ds} \\ V_{dr} &= R_r I_{dr} + \frac{d}{dt}\phi_{dr} - \omega_r \phi_{qr} \\ V_{qr} &= R_r I_{qr} + \frac{d}{dt}\phi_{qr} + \omega_r \phi_{dr} \end{aligned} \quad (5)$$

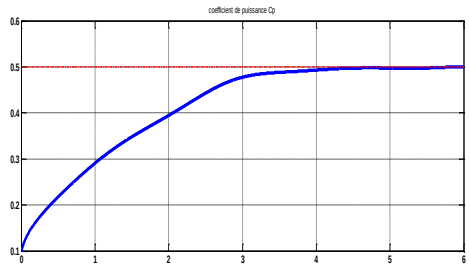

Figure 1. Aerodynamic power coefficient variation Cp against tip speed ratio λ and pitch angle β

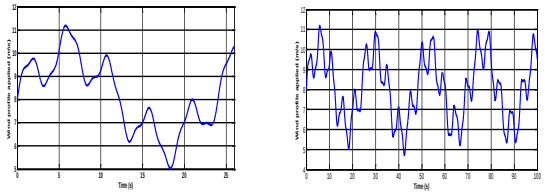

Figure 2. Wind turbine profile

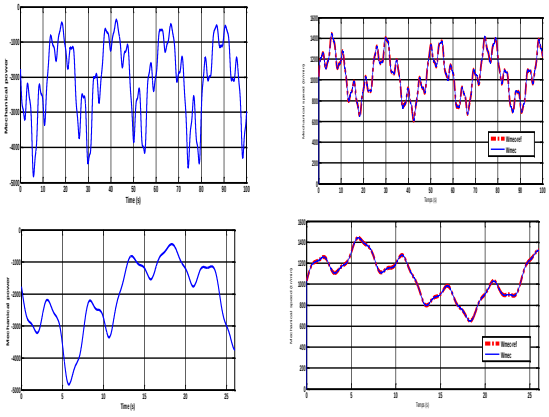

(a) (b)

Figure 3. (a) Power with MPPT, **(b)** Mechanical Wind Speed

With: $\omega_r = (\omega_s - \omega)$
Stator and rotor flux:

$$\begin{aligned} \phi_{ds} &= L_s I_{ds} + M I_{dr} \\ \phi_{qs} &= L_s I_{qs} + M I_{qr} \\ \phi_{dr} &= L_r I_{dr} + M I_{ds} \\ \phi_{qr} &= L_r I_{qr} + M I_{qs} \end{aligned} \quad (6)$$

The electromagnetic torque is done as:

$$C_e = p\frac{M}{L_s}(I_{dr}.\phi_{qs} - I_{qr}.\phi_{ds}) \quad (7)$$

And it's associated motion as:

$$C_e - C_r = J\frac{d\Omega}{dt} \quad (8)$$

4. FIELD ORIENTED CONTROL OF DFIG

In order to achieve independent control of active and reactive power, a two-phase *d-q* rotating reference frame is chosen related to the stator field [3]. Such as:

$$\phi_{ds} = \phi_s = L_s I_{ds} + M I_{dr} \Rightarrow I_{ds} = \frac{\phi_s}{L_s} - \frac{M}{L_s} I_{dr} \quad (9)$$

$$\phi_{qs} = 0 = L_s I_{qs} + M I_{qr} \Rightarrow I_{qs} = -\frac{M}{L_s} I_{qr}. \quad (10)$$

The stator voltage will be expressed by:

$$V_{ds} = 0 \text{ and } V_{qs} = V_{ds} \sim \omega_s \phi_s \quad (11)$$

For medium and high power generators used in wind turbine, the stator resistance R_s can be neglected where the transversal components I_{rq}, I_{rd} of the rotor currents, controls the P_s. Q_s respectively. To obtain Equations (12) and (13) presented below we use Equations (9),(10) and (11) we find:

$$P_s = V_{qs} I_{qs} + V_{ds} I_{ds} = V_{qs} I_{qs} = -V_s \frac{M}{L_s} I_{qr} \quad (12)$$

$$Q_s = V_{qs} I_{ds} - V_{ds} I_{qs} = \frac{V_s^2}{\omega_s L_s} - V_s \frac{M}{L_s} I_{dr} \quad (13)$$

The arrangement of the Equations (5) and (6) gives the expressions of the voltages according to the rotor currents:

$$V_{dr} = R_r I_{dr} + \sigma L_r \frac{d}{dt} I_{dr} - g\omega_s \sigma L_r I_{qr} \quad (14)$$

$$V_{qr} = R_r I_{qr} + \sigma L_r \frac{d}{dt} I_{qr} + g\frac{M}{L_s} V_s + g\omega_s \sigma L_r I_{dr} \quad (15)$$

In this state we can find the derivative rotor currents as shown in Equations (16) and (17):

$$\dot{I_{dr}} = -\frac{1}{\sigma T_r} I_{dr} + g\omega_s I_{qr} + \frac{1}{\sigma L_r} V_{dr} \quad (16)$$

$$\dot{I_{qr}} = -\frac{1}{\sigma}\left(\frac{1}{T_r} + \frac{M^2}{L_s T_s L_r}\right) I_{qr} - g\omega_s I_{dr} + \frac{1}{\sigma L_r} V_{qr} \quad (17)$$

With: $T_r = \frac{L_r}{R_r}$, $T_s = \frac{L_s}{R_s}$, $\sigma = 1 - \frac{M^2}{L_s L_r}$, $g = \frac{\omega_s - \omega}{\omega_s}$

Figure 4 present a description of the DFIG model used in this paper. Figure 5 describes a field oriented control applied to DFIG for wind power system. In the next section, a robust indirect sliding mode control is applied to DFIG.

5. INDIRECT SLIDING MODE CONTROL

Indirect sliding mode control (ISMC) possesses strengthen robustness and has been successfully applied in wind energy conversion system (WECS) [4].

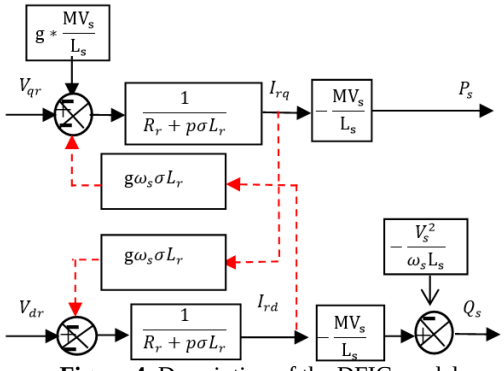

Figure 4. Description of the DFIG model

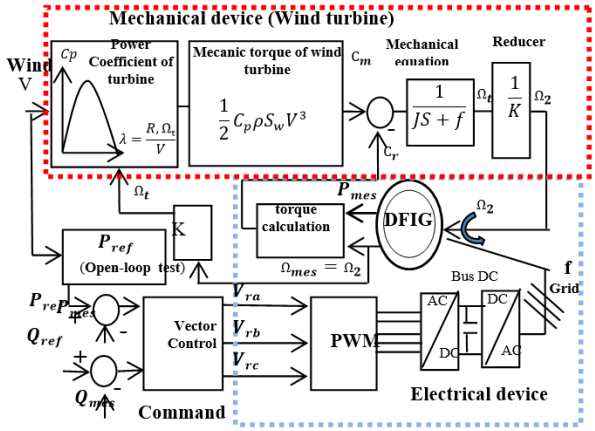

Figure 5. Vector-control structure for wind power system

The indirect sliding mode is to take into account the coupling terms and to compensate for them by performing a system comprising two loops for controlling the powers and the rotor currents. This method called indirect method.

Thus, the relationships between stator powers and rotor currents are given by:

$$I_{qr}^{*} = -\frac{L_s}{MV_s} P_s^{ref} \tag{18}$$

$$I_{dr}^{*} = \frac{V_s}{M\omega_s} - \frac{L_s}{MV_s} Q_s^{ref} \tag{19}$$

The rotor currents have to track appropriate current references, so, a sliding mode control based on the above Park reference frame is used.

5. 1. Choice of Sliding Surface The sliding surfaces *S(x)*. representing the error between the measured and reference rotor currents are given by this relation:

$$S(I_{qr}) = I_{qr}^{*} - I_{qr} \tag{20}$$

$$S(I_{dr}) = I_{dr}^{*} - I_{dr} \tag{21}$$

5. 2. Condition of Convergence Consequently, for a sliding surface S (I_{rq},I_{rd}), the active and reactive power would converge exponentially towards their references. So, to track P_s and Q_s. The effectiveness of a sliding mode control is conditioned by checking Lyaponuv'attractivity relationship [8], given by:

$$S(x)\dot{S}(x) \le 0 \tag{22}$$

5. 3. Sliding Mode Control Algorithm To control active power, we put r =1(*relative degree of the number of derivative times of the control surface to get the control LAW*), so the expression of the control of surface derivative to control active power and reactive power are given by:

$$\dot{S}(I_{qr}) = \dot{I}_{qr}^{*} - \dot{I}_{qr} \tag{23}$$

$$\dot{S}(I_{dr}) = \dot{I}_{dr}^{*} - \dot{I}_{dr} \tag{24}$$

Substituting the expression of $\dot{I}_{qr}$, $\dot{I}_{dr}$ equations shown in (16) and (17) in Equation (23) and (24), we obtain:

$$\dot{S}(I_{qr}) = \dot{I}_{qr}^{*} - (-\frac{1}{\sigma}\left(\frac{1}{T_r} + \frac{M^2}{L_s T_s L_r}\right) I_{qr} - g\omega_s I_{dr} + \frac{1}{\sigma L_r} V_{qr}) \tag{25}$$

$$\dot{S}(I_{dr}) = \dot{I}_{dr}^{*} - (-\frac{1}{\sigma T_r} I_{dr} + g\omega_s I_{qr} + \frac{1}{\sigma L_r} V_{dr}) \tag{26}$$

The sliding mode law can be given as bellow:

$$V_{qs} = V_{qr}^{eq} + V_{qr}^{n} \tag{27}$$

$$V_{dr} = V_{dr}^{eq} + V_{dr}^{n} \tag{28}$$

During the sliding mode and in permanent regime, we have:

$$S(I_{qr}) = 0\ ,\dot{S}(I_{qr}) = 0\ ,\ V_{qr}^{n} = 0 \tag{29}$$

$$S(I_{dr}) = 0\ ,\dot{S}(I_{dr}) = 0, V_{dr}^{n} = 0 \tag{30}$$

Where the equivalent controls are:

$$V_{qr}^{eq} = \dot{I}_{qr}^{*} + \frac{1}{\sigma}\left(\frac{1}{T_r} + \frac{M^2}{L_s T_s L_r}\right) \dot{I}_{qr} + g\omega_s I_{dr})\sigma L_r \tag{31}$$

$$V_{dr}^{eq} = (\dot{I}_{dr}^{*} + \frac{1}{\sigma T_r} I_{dr} - g\omega_s I_{qr})\sigma L_r \tag{32}$$

Therefore, the correction factor are given by:

$$V_{qr}^{n} = k_{qr} sign(S(I_{qr})) \tag{33}$$

$$V_{dr}^{n} = k_{dr} sign(S(I_{dr})) \tag{34}$$

Where:k_{dr} , k_{qr} positive constant
according to Equations (31), (32), (33) and (34) we can find our control law mentioned in Equations (27) and (28) respectively.

For more description Figure 6 present an indirect sliding mode control combined with DFIG.

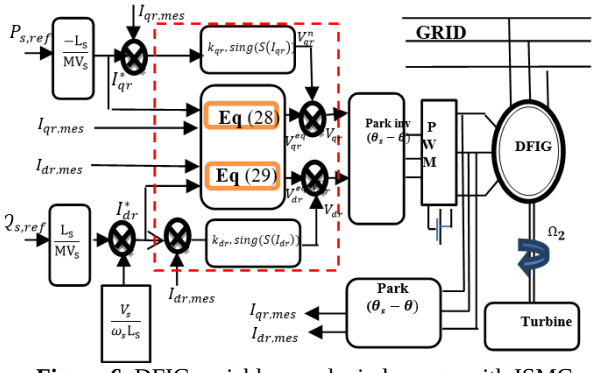

Figure 6. DFIG variable speed wind energy with ISMC

In order to evaluate this strategy, simulations results are presented and discussed in the next section.

6. SIMULATION RESULTS

The DFIG used in this work is a 4kW; his nominal parameters are indicated in Tables 1 and 2:

In this work we are interested to present two kind of simulation results. The first case is the implementation of the control law with a fixed speed (without turbine). While in the second case, the simulation study has been carried out with variable speed (with the presence of turbine and wind profile).

6. 1. First Case: Fixed Speed In the Figures (7, 8, 9, 10) we present a qualitative comparison of simulation results between the various steps for active and reactive power suggested in this on work. For a small speed wind the control device ensures the optimization of the power extracted by maintaining the reactivity power coefficient from the turbine its maximum value. Simulation results show clearly the improvement of active and reactive power demand obtained by applying sliding mode control in term of time response (2s) and Excellent reference tracking accuracy than those obtained using traditional FOC.

TABLE 1. Parameters of the DFIG [9]

Rated Power:	4 kWatts
Stator Resistance:	Rs = 1.2Ω
Rotor Resistance:	Rr = 1.8Ω
Stator Inductance:	Ls = 0.1554 H.
Rotor Inductance:	Lr = 0.1568 H.
Mutual Inductance:	M = 0.15 H.
Rated Voltage:	Vs = 220/380 V
Number of Pole pairs:	P= 2
Rated Speed:	N=1440 rpm
Friction Coefficient:	fDFIG=0.001 N.m/rad
The moment of inertia	J=0.2 kg.m^2

TABLE 2. Parameters of the turbine [9]

Number of pale	Np= 3
Blade diameter	R_T= 3m
Gain:	G=5.4
The moment of inertia	Jt=315 kg.m^2
Friction coefficient	ft=0.024 N.m/rad
Air density:	ρ=1.22 Kg/m^3

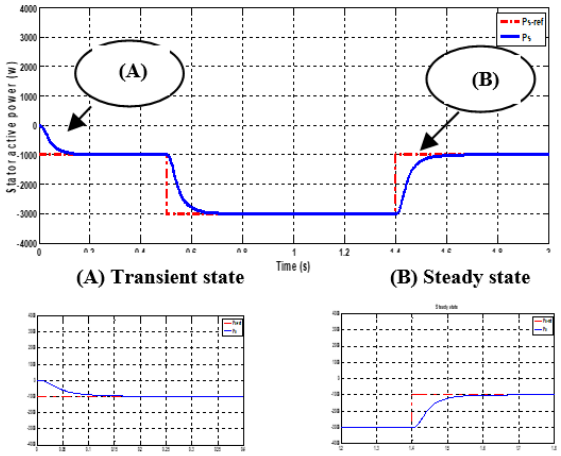

Figure 7. Stator active power for FOC

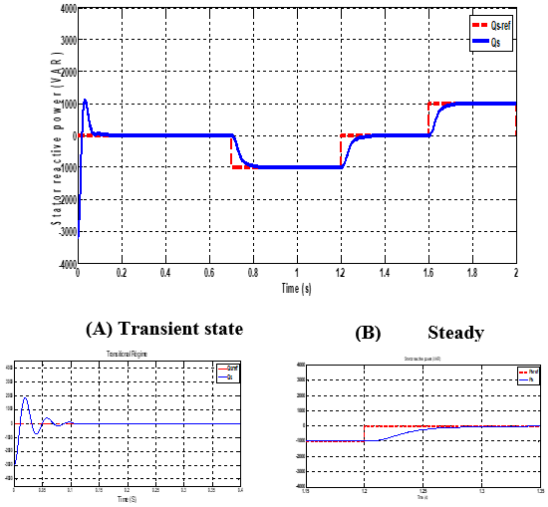

Figure 8. Stator reactive power for FOC

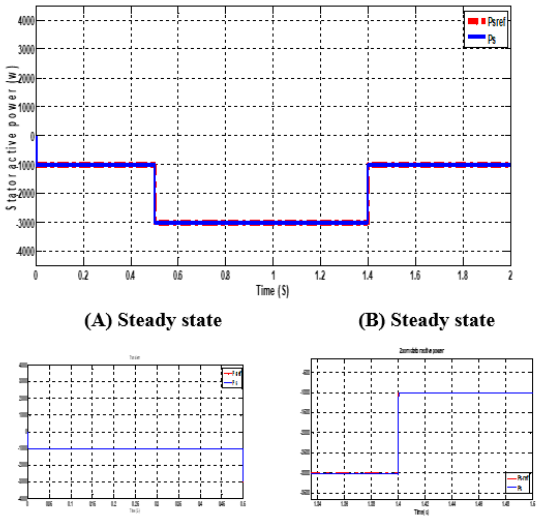

Figure 9. Stator active power for ISMC

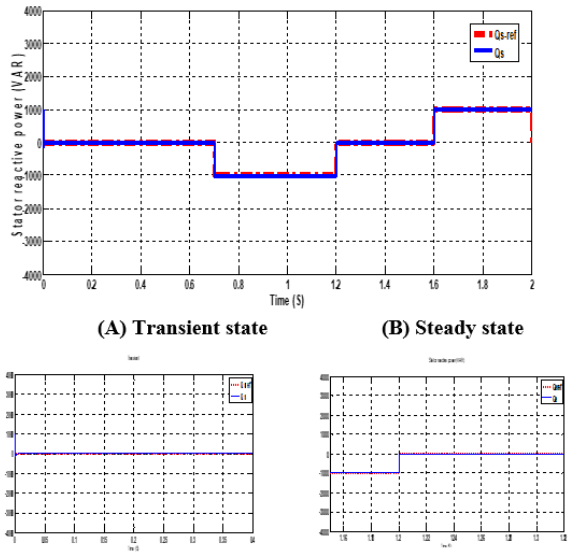

Figure 10. Stator reactive power for ISMC

We notice here, in case of step change, that the sliding mode control transient responses of both active and reactive powers present no overshoot where as the steady state justified by Zoom of transient and steady state.

6. 2. Second Case: Wind Profile For this purpose a wind speed profile (Figure 2) has been applied to the turbine to observe the capability of our controllers to act against this kind of disturbance, where the generated mechanical speed and the obtained power coefficient, C_p are shown in Figures 1 and 3 respectively.

Figures bellow show the variations of the various parameters (active and reactive power, rotor and stator currents) when the inverter (PWM) is taken into account in simulations.

We notice that the stator active power is negative what means that DFDFIG DFIG produces energy and provided to the network. Thus the reactive power is null, which enables us to have a unit power-factor.

Moreover, the increase of the wind speed generates increases on the level of the stator and rotor currents

Figures 11 and 12 show the simulation results of active and reactive power for both vector and sliding mode control respectively it is clear that the measure powers (active and reactive) have good chase with high performance (little error, and short response time) as for as their reference powers.

First it could be noticed the best performances and excellent rejection of disturbance and a satisfactory tracking performance respectively of active and reactive power of sliding mode control compared to vector control in steady state as well as in transient. In addition in case of disturbance and time response, the simulation results of the sliding mode control show no overshoot and the overall system behaves like a first order system while in the vector control, it behaves like a second order system with a significant overshoot.

In Figures 13, 14, 15 and 16 are the time evolution of stator and rotor currents respectively in both transient and steady state for vector and ISMC. We can note less overshoot and oscillations of ISMC compared with FOC.

Figure 17 present the active and reactive errors for FOC. We observe a low error of active and reactive power nearly:$-500/Var \leq \Delta P_S, \Delta Q_S \leq +500/Var$

Figure 18 present the active and reactive errors for ISMC. We observe a low error of active and reactive power nearly:$-10/Var \leq \Delta P_S, \Delta Q_S \leq +10/Var$

In Figure 19 it is given the time evolution of the phase stator current versus phase voltage respectively. It is clearly shown that the overall system operate at a unity power factor.

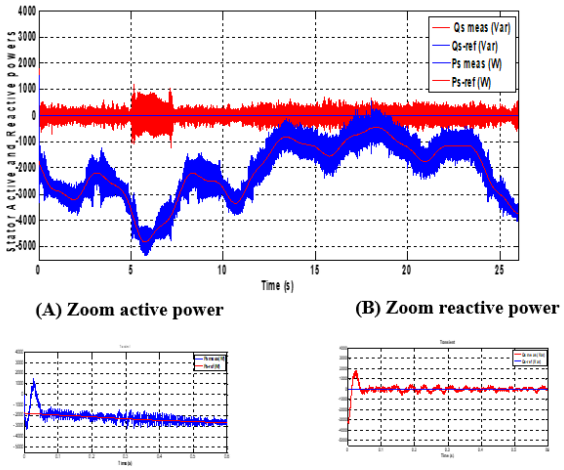

Figure 11. Stator active and reactive powers for FOC

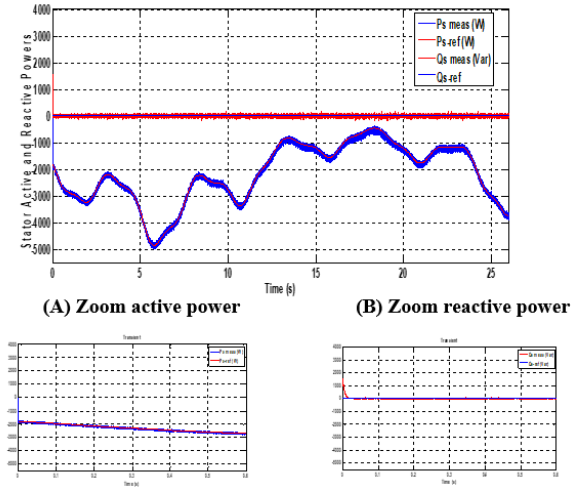

Figure 12. Stator active power for ISMC

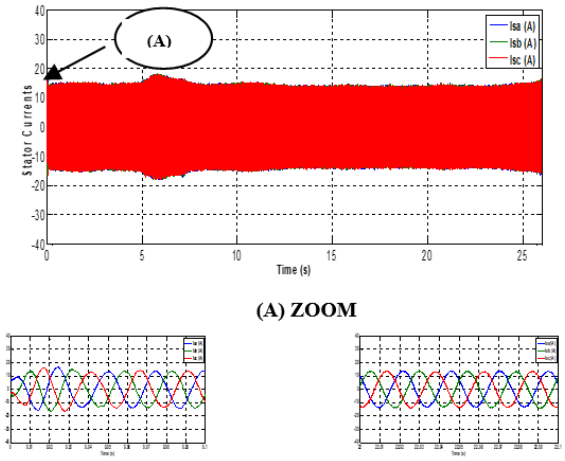

Figure 13. Stator currents for FOC

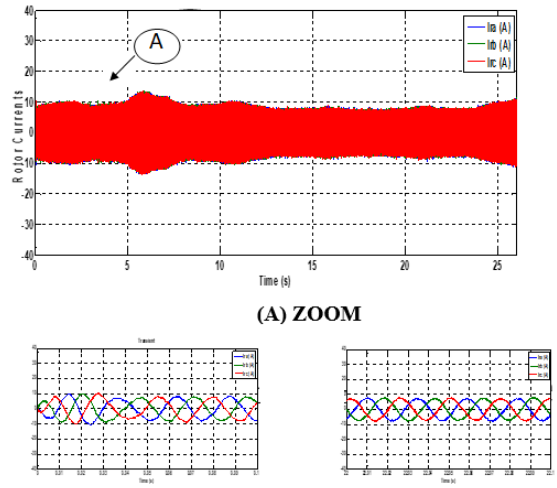

Figure 14. Rotor currents for FOC

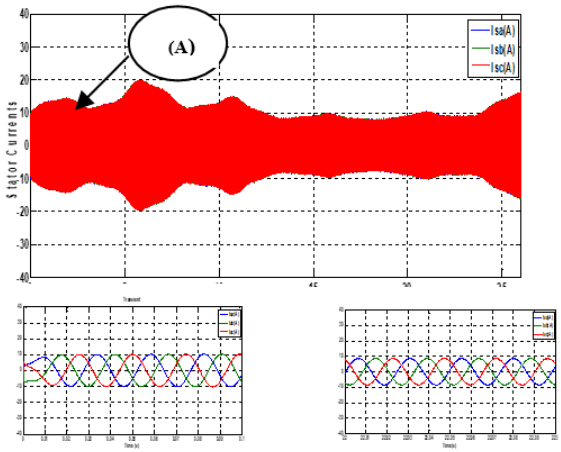

Figure 15. Stator currents for ISMC

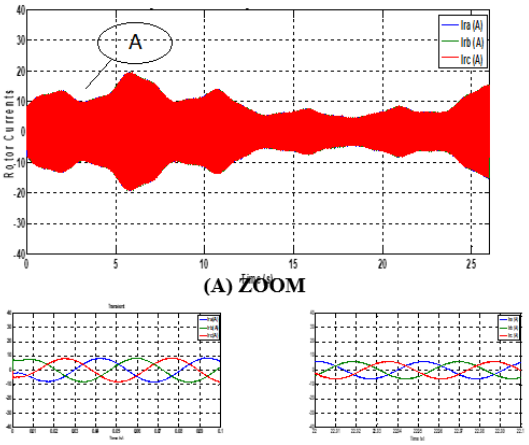

Figure 16. Rotor currents for ISMC

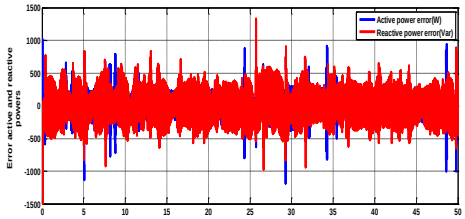

Figure 17. Tracking errors of stator active and reactive powers

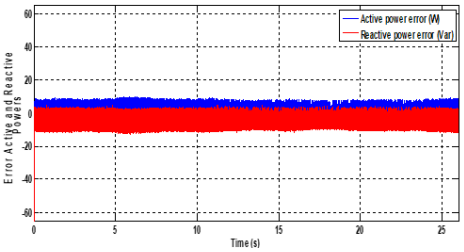

Figure 18. Tracking errors of stator active and reactive powers

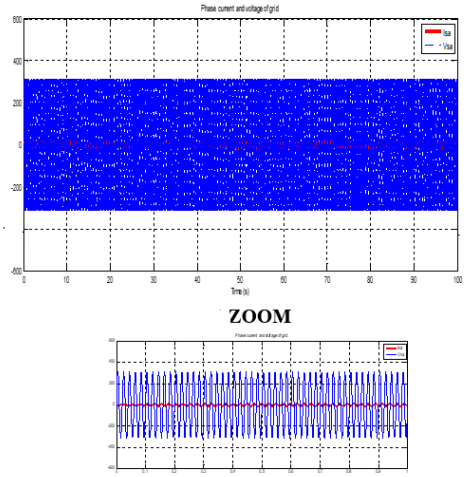

Figure 19. Phase stator current and phase voltage

6. 3 Robustness Test Figures 20 and 21 show the response of the stator active and reactive powers of the DFIG applied to the sliding mode control for a variation of + 50% of the nominal value of the rotor resistance R_r and inductance L_r. From these figures, we can see that the variation of the R_r and L_r does not cause any effect on all stator active and reactive powers, and this shows the robustness of the control by sliding mode against the variation of the R_r and L_r. In addition, decoupling is not affected by this variation.

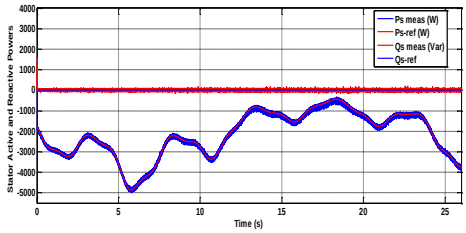

Figure 20. Robustness test with 50% of R_r variation

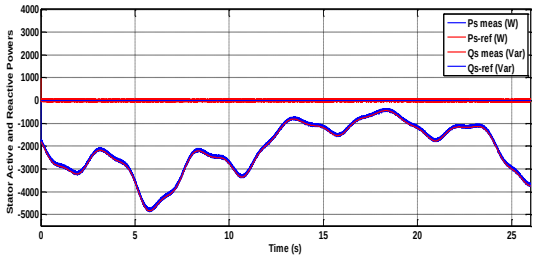

Figure 21. Robustness test with 50% of L_r variation

7. CONCLUSION

Based to simulation results of FOC and ISMC for active and reactive power control of a DFIG, using the MPPT strategy. The proposed indirect sliding mode control strategy presents robust and simple algorithm that has the advantage of being easily implantable in a calculator. The obtained results clearly show the indirect sliding mode control approach effectiveness in terms of dynamic and steady state operation, robustness in a short response perfect decoupled of active and reactive powers and power extraction maximization compared to FOC.

With an appropriate choice of the control law, the results we have obtained are interesting for the application of wind energy to ensure robustness and the quality of the energy produced. The control based on sliding mode control not only enhances the overall quality of the delivered power but also ensure functioning at unity power factor.

8. REFERENCES

1. Salehi, M. and Davarani, R.Z., "Effect of different turbine-generator shaft models on the subsynchronous resonance phenomenon in the double cage induction generator based wind farm", ***International Journal of Engineering-Transactions B: Applications***, Vol. 29, No. 8, (2016), 1103-1111.
2. Hamidi, H., Mortazave, H. and Salahshoor, A., "Designing and modeling a control system for aircraft in the presence of wind disturbance", ***International Journal of Engineering-Transactions C: Aspects***, Vol. 30, No. 12, (2017), 1856-1862.
3. Aroussi, H., Ziani, E. and Bossoufi, B., "Robust control of a power wind system based on the double fed induction generator (DFIG)", ***Journal of Automation & Systems Engineering JASE***, Vol. 9, No. 3, (2015), 156-166.
4. Rouabhi, R., Abdessemed, R., Chouder, A. and Djerioui, A., "Power quality enhancement of grid connected doubly-fed induction generator using sliding mode control", ***International Review of Electrical Engineering***, Vol. 10, (2015), 266-276.
5. Boualouch, A., Essadki, A., Nasser, T., Boukhriss, A. and Frigui, A., "Power control of dfig in wecs using backstipping and sliding mode controller", ***International Journal of Electrical Computer Energetic Electronic and Communication Engineering***, Vol. 9, (2015), 612-618.
6. Karami-Mollaee, A., "Adaptive fuzzy dynamic sliding mode control of nonlinear systems", ***International Journal of Engineering-Transactions B: Applications***, Vol. 29, No. 8, (2016), 1075-1086.
7. Vali, M., Rezaie, B. and Rahmani, Z., "Designinga neuro-sliding mode controller for networked control systems with packet dropout", ***International Journal of Engineering-Transactions A: Basics***, Vol. 29, No. 4, (2016), 490-499.
8. Mechter, A., Kemih, K. and Ghanes, M., "Sliding mode control of a wind turbine with exponential reaching law", ***Acta Polytechnica Hungarica***, Vol. 12, No. 03, (2015), 167-183.
9. Drid, S., "Contribution à la modélisation et à la commande robuste d'une machine à induction double alimentée à flux orienté avec optimisation de la structure d'alimentation: Théorie et expérimentation", PhD Thesis, University of Batna, Algeria, (2005).

Improvement Performances of Active and Reactive Power Control Applied to DFIG for Variable Speed Wind Turbine Using Sliding Mode Control and FOC

T. Douadi[a], Y. Harbouche[a], R. Abdessemed[a], I. Bakhti[b]

[a] LEB – Research Laboratory, Department of Electrical Engineering, Mostefa Benboulaid-Batna 2 University, Algeria
[b] Laboratory of Electromagnetic Induction and Propulsion Systems, Department of Electrical Engineering, Batna University, Algeria

P A P E R I N F O

Paper history:
Received 08 April 2018
Received in revised form 26 July 2018
Accepted 17 August 2018

Keywords:
Doubly Fed Induction Generator
Field Oriented Control
Indirect Sliding Mode
Wind Energy
Pulse with Modulation PWM

چکیده

این مقاله با کنترل نیروی فعال و واکنش پذیر از ژنراتور القایی دوگانه (DFIG) برای توربین بادی متغیر سرعت را بررسی می کند. برای کنترل جداگانه نیروی فعال و راکتیو تولید شده توسط یکDFIG ، کنترل میدان (FOC) و کنترل غیر مستقیم کشویی (ISMC) ارائه شده است. این کنترل های غیر خطی بر اساس توپولوژی، هزینه و کارایی مقایسه می شوند. سهم اصلی این کار براساس زمان کوتاه پاسخ با همگرایی عالی و جدا شدن بالا بین قدرت فعال و راکتیو در یک بخش و در قسمت دوم، ما مزایای استفاده از مدل غیر مستقیم DFIG را به مفهوم کنترل حالت غیر مستقیم لغزشی تعریف می کنیم با استفاده از رابطه بین قدرت استاتور و جریان روتور. نتایج شبیه سازی عملکرد خوبی در مورد ردیابی مراجع در حالت گذرا و پایدار نشان داده شده است و اثربخشی کنترل حالت کشویی را برای پیگیری ارجاع داده شده با استفاده از اینورتر PWM نشان می دهد.

***doi**: 10.5829/ije.2018.31.10a.11*